Analytical Methods

Accepted Manuscript

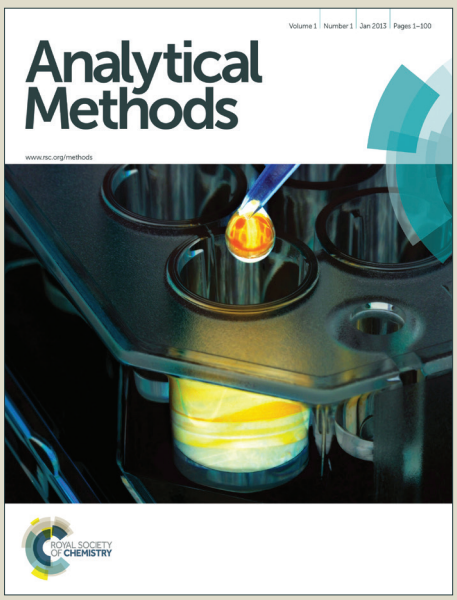

ROYAL SOCIETY OF CHEMISTRY

www.rsc.org/methods

Sensitive voltammetric determination of neohesperidin dihydrochalcone based on SWNTs modified glassy carbon electrode

Lingxi Yang [a], Lu Wang [a,b], Kunjing Li [a], Baoxian Ye*[a]

a College of Chemistry and Molecular Engineering, Zhengzhou University, Zhengzhou 450001, *PR* China

b Department of Environmental Engineering and Chemistry, Luoyang Institute of Science and Technology, Luoyang 471023, PR China

Received (in XXX, XXX) Xth XXXXXXXXX 20XX, Accepted Xth XXXXXXXXX 20XX
DOI: 10.1039/b000000x

Abtract:

A new voltammetric sensor, based on single-walled carbon nanotubes (SWNTs) modifid glassy carbon electrode, was established and used for determination of neohesperidin dihydrochalcone (NHDC). The electrochemical character of NHDC on this sensor was studied systematically by cyclic voltammetry and some kinetics parameters were calculated for the first time. Compared with bare GCE, the proposed sensor exhibited excellent redox activity towards NHDC, and a new voltammetric analytical method for NHDC was proposed with a wide liner range from 5×10^{-8} mol/L to 8×10^{-6} mol/L and a low detection limit of 2×10^{-8} mol/L. In addition, a reasonable mechanism was also proposed and discussed. Finally, the developed method was successfully applied to quantitative determination of NHDC in beverages with high accuracy and satisfactory recovery results.

Introduction

Neohesperidin dihydrochalcone (NHDC, Fig.1) is an intensely sweet substance, which is produced by catalytic hydrogenation of neohesperidin, the predominant flavanone glycoside of bitter oranges. In the early 1960s, it is found to have strong sweetness by Horowitz, which is 20 times sweeter than saccharin and 1500-1800 times than sucrose on molar basis [1]. Thus, NHDC has been evaluated for use as a low caloric artificial sweetener in various foods and beverages [2]. Because of the delayed onset and long lingering menthol-licorice, NHDC can reduce the sensitivity to bitter taste for human and animals, and has widely been applied in pharmaceuticals [3] and feedstuff [4] as a bitterness blocker and flavor enhancer. Besides, it can also offer treatment for diabetes mellitus effectively [5]. However, as a kind of food additives, the maximum level permitted for NHDC was 5mg/kg declared by The Scientific Committee for Foods of the European Community in 1987. At present, the evaluation and research for NHDC mainly concentrate on its synthetic and extraction method [6], pharmacological activities [7-8] as well as stability in samples [9], Thus, a simple and rapid analytical assay for this compound became desirable. Some analytical techniques have been established for determining NHDC, including high-performance liquid chromatography (HPLC) [10], LC-MS [11-12] and capillary electrophoresis [13]. We have awared that there has been few report regarding the

electrochemistry and voltammetric determination of NHDC so far. Furthermore, the pharmacological action and reaction mechanism of NHDC are not observed using these methods. Electrochemical methods have attracted more and more attentions due to the advantages of fast response, easy operation, time-saving, low-cost instrumentation, high sensitivity and excellent selectivity comparing with the existing methods. More importantly, the techniques also help for identifying the redox of compounds and provide important information about pharmacological actions.

Carbon Nanotubes (CNTs, called bucky tube), which were generated by rolling a single or several layers of graphite into a seamless and hollow cylinder, has aroused widespread concern since their appearance in 1990. Based on the number of carbon atom layers, it can be divided into multi-walled carbon nanotubes (MWNTs) and single-walled carbon nanotubes (SWNTs) [14-15]. Because of its high electrical conductivity, large specific surface area, good electrical characteristics and good mechanical properties, CNTs have been widely employed in electrochemistry analysis, especially in the fabrication of electrochemical voltammetric sensors and biosensors [16-17].

In the present approach, the SWNTs was employed again for modifying on glassy carbon electrode (SWNTs/GCE). As a voltammetric sensor, it has high sensitive response for NHDC. Therefore, a simple assay was established for determination of NHDC with high sensitivity and selectivity, as well as wider linear range. The influence factors and kinetic parameters of electrode reaction of NHDC on SWNTs/GCE were investigated in detail. A reasonable mechanism of electrode reaction was proposed for the first time. Furthermore, the proposed voltammetric sensor was applied to the determination of NHDC in beverages with good accuracy and satisfactory recovery.

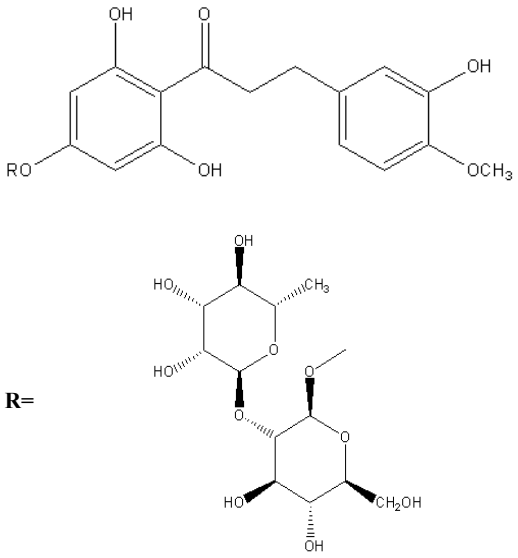

Fig. 1 The chemical structure of NHDC

Experimental

Apparatus and reagents

RST3000 Electrochemical analyzer (Zhengzhou Shiruisi Instrument Technology Co., Ltd., China) was employed for electrochemical techniques. A conventional three-electrode system consisting of an Ag/AgCl reference electrode, a platinum auxiliary electrode, and a GCE or modified GCE working electrode was used. All the pH measurements were carried out with a pHS-2C Digital pH meter (Shanghai Lida, Shanghai, China) equipped with a combined glass electrode, which was calibrated regularly with standard buffer solutions (pH 2.0 to 7.0) at 25 ± 0.1□

All reagents were of analytical grade and were used as received. SWNTs (95% purity) and MWNTs (95% purity, 8 nm diameter, 30 mm length) were purchased from Beijing Nachen S&T Ltd, China. Neohesperidin dihydrochalcone

(NHDC) was purchased from Aladdin Chemistry Co., Ltd. (Shanghai, China). Phosphate buffer solution (pH 3.0) by mixing the stock solutions of 0.1 mol L^{-1} NaH_2PO_4 and Na_2HPO_4 was used as the supporting electrolyte. A standard stock solution of NHDC (1×10^{-3} mol L^{-1}) was prepared with ethanol and kept in the dark under 4□. Double distilled water was used for all preparation. All electrochemical experiments were carried out at room temperature.

Fabrication of SWNTs modified electrode

Prior to the surface modification, purification and carboxylation of the SWNTs was carried out according to the methods described in references [18]. Functionalized SWNTs (2.0 mg) were then dissolved in DMF solution and sonicated in an ultrasonic bath for 3 h to obtain a uniformly black suspension of 1.0 mg mL^{-1}. Before use, the working electrode was polished with alumina (0.3 μm) water slurry, rinsed, sonicated in ethanol and doubly distilled water respectively, each for 10min. The SWNTs modified GCE was fabricated by dropping the suspension of SWNTs in DMF (10 μL) on the fresh GCE surface and then evaporating the solvent naturally. For a comparison, a MWNTs modified GCE was prepared using the same method (the MWNTs were pretreated using the method for SWNTs) and denoted as MWNTs/GCE.

Analytical procedure

Firstly the modified GCE was subjected to stabilization in 3.0 PBS by cyclic sweep between potential of 0.0 V and 0.9 V for 10 cycles at 50 mV/s. Then a appropriate volume of NHDC standard solution was added into the electrochemical cell. After accumulation for 180 s at open circuit with stirring, the quantitative determination of NHDC was performed by applying a positive-going cycle voltammetry (CV) and linear sweep voltammetry (LSV) scan. In order to obtain a renew electrode surface, the modified electrode was transferred to 0.05mol L^{-1} NaOH solution by successive sweeping of two cycles between 0.0V and 0.9V.

Results and discussion

Characterization of SWNTs/GCE

To evaluate the charge transfer properties on the surface of the modified electrode, cyclic voltammograms of the GCE (curve a), SWNTs/GCE (curve b) were obtained in 1×10^{-3} mol L^{-1} $K_3[Fe(CN)_6]$ solution containing 0.1 mol L^{-1} KCl. As displayed in Fig. 2, a well-defined CV, characteristic of diffusion-limited and reversible electron transfer redox process, was observed at bare GCE with i_{pa} = 10.76 μA, i_{pc} = 10.47 μA and peak-to-peak separation of 65 mV. At the SWNTs modified electrode, the redox peak currents apparently increased to i_{pa} = 43.30 μA, i_{pc} = 37.30 μA with larger charging current. The rise in current clearly indicated the role of SWNTs in the increase of the conductivity and effective surface area.

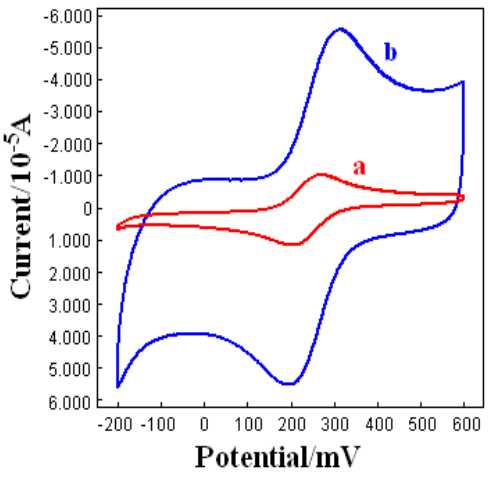

Fig. 2 Cyclic voltammograms of $Fe(CN)_6^{3-}$ (1×10^{-3} mol L^{-1}) at bare GCE **(a)** and SWNTs/GCE **(b)** Supporting electrolyte: 0.1mol L^{-1} KCl. Scan rate: 50 mV s^{-1}

For further characterization of the modified electrode, electrochemical impedance spectroscopy (EIS) was also performed. In the Nyquist plot of EIS, the semicircle part at higher frequencies corresponds to the electron transfer limited process, and the linear part at lower frequencies corresponds to the diffusion process. Therefore, the electron-transfer resistance (Ret) can be used to denote the impedance of electrode surface. Fig. 3 presented the Nyquist of EIS at bare GCE (a) and SWNTs/GCE (b) in 5×10^{-3} mol L^{-1} $[Fe(CN)_6]^{3-/4-}$ solution containing 0.2 mol L^{-1} KCl. It can be seen that the spectrum of the bare GCE exhibited a very small semicircle (Ret=36.40 Ω) at the high frequency region relating to the interfacial electron transfer resistance. In contrast, the resistance value decreased to an almost straight (Ret=23.96Ω) at SWNTs/GCE, indicating that the impedance characteristics of the modified electrode was controlled by the diffusion in all frequency regions. This result was in accordance with the cyclic voltammetry token and both of them contributed to the excellent charge conductibility of SWNTs.

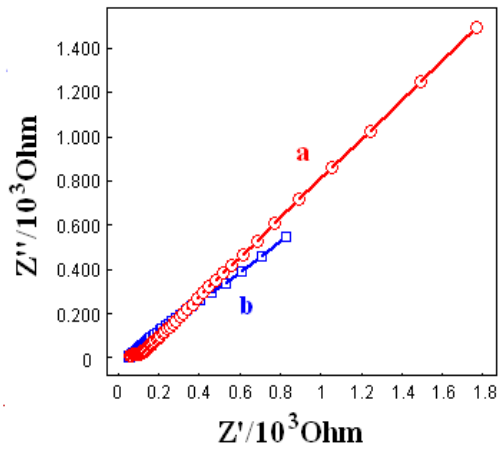

Fig. 3 Nyquist plots for electrochemical impedance measurements at bare GCE **(a)**, SWNTs/GCE **(b)** in 5×10^{-3} mol L^{-1} $Fe(CN)_6^{3-/4-}$ containing 0.2mol L^{-1} KCl. Frequency range: 1.0 MHz to 0.01 Hz

Electrochemical Behavior of NHDC at SWNTs modified electrode

Fig. 4 shows the voltammograms of NHDC (5×10^{-6} mol L^{-1}) at bare GCE (curve a), MWNTs/GCE (curve b) and SWNTs/GCE (curve d) in 0.1mol L^{-1} PBS (pH=3.0). Every scan was performed for two cycles. A background voltammogram at SWNTs/GCE was presented as curve c in Fig. 4. At the bare GCE, NHDC exhibited a poor electrochemical response in potential window between 0.0 V and 0.9 V. At the SWNTs/GCE, NHDC showed a well-defined irreversible anodic peak with E_p=0.666 V (P1) and a cathodic peak with E_p = 0.388V (P2) during the first cyclic scan. In successive second cycle, a new sensitive anodic peak with E_p = 0.430V (P3) was observed and the current of P1 decreased. The P2 remained same as in the first cycle. In the case of MWNTs/GCE, the electrode reaction of NHDC was the same as that at SWNTs/GCE with smaller

peak currents and charging current (Fig. 4, curve b). These results also demonstrated that the conductibility of MWNTs was poor comparing with that of SWNTs. From the reaction character of NHDC, we preliminary estimated that the P2 and P3 were a pair of redox peaks and their active group came from the oxidation product of P1.

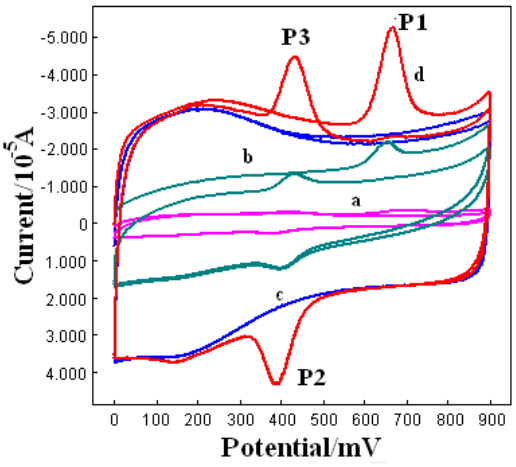

Fig. 4 Cyclic voltammograms of NHDC (5×10^{-6} mol L^{-1}) at bare GCE **(a)**, MWNTs/GCE **(b)**, SWNTs/GCE **(c)** and SWNTs/CGE in blank solution **(d)**. Supporting electrolyte: 0.1 mol L^{-1} PBS (pH =3.0), scan rate: 50 mV s^{-1}, Open-circuit accumulation time: 180 s

To further assess the electrochemical properties of NHDC, we controlled the scan potential window with different ranges. Firstly, the potential window was controlled between 0.0 and 0.50 V for 4 cyclic scans, and no redox peaks were observed (shown in Fig. 5A). Secondly, when the potential window was set between 0.50 V and 0.90 V for 4 cyclic scans, P1 was appearance in the first cycle and no any redox peaks were observed in following scans (Fig. 5B). Thirdly, the potential window was controlled between 0.0V and 0.90V, and the initial potential was set at 0.50 V going negatively for 4 cycles (Fig. 5C). As expected, the P2 was not observed in first cycle and the three peaks were obtained just as the curve d in Fig. 3. This result confirmed the above prediction. Finally, four consecutive cyclic scans were performed in the above solution with potential window between 0.0V and 0.90V, the P1 disappeared after the first cycle and the peak currents and potentials of P2 and P3 almost kept unchanged in following scans (Fig. 5D)

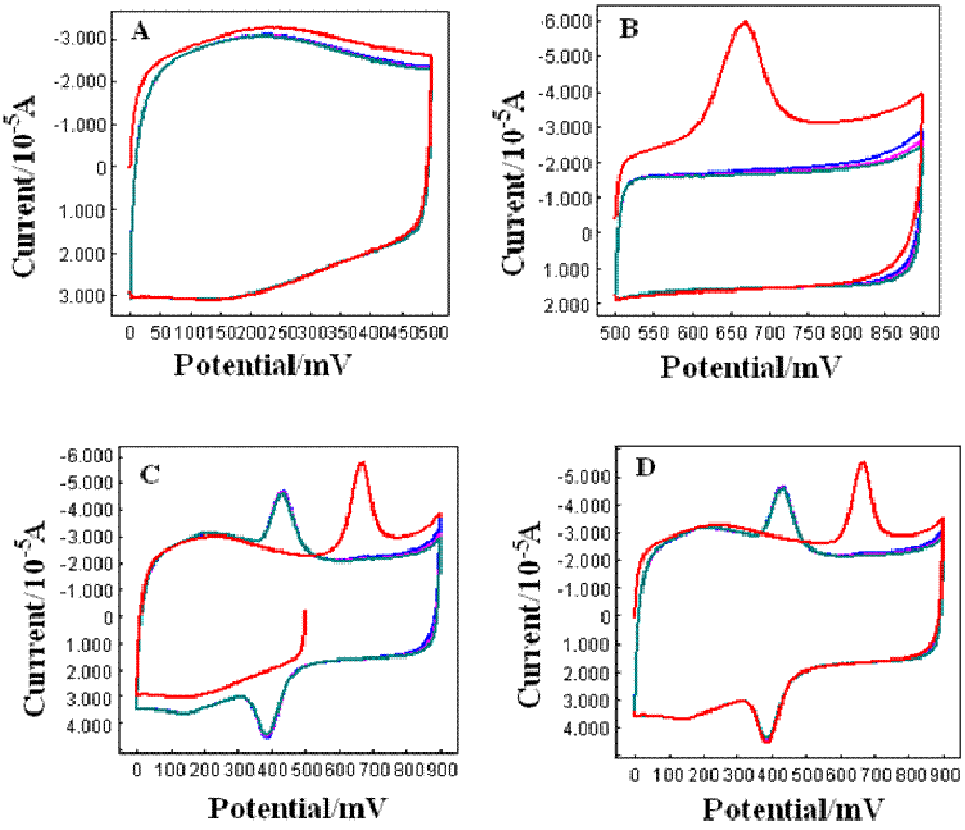

Fig. 5 Cyclic voltammograms of NHDC (5×10^{-6} mol L^{-1}) in 0.1mol L^{-1} PBS (pH=3.0) with different potential window. Other conditions were same as Fig. 4

The effect of electrolyte and pH

The types of supporting electrolytes played a key role in the voltammetric response of NHDC. To get the best response, the influences of supporting electrolytes were investigated in phosphate buffer, Britton-Robinson, acetate buffer, sulfuric acid and muriatic acid solutions spiked with 3×10^{-6} mol L^{-1} NHDC. It was noted that higher peak current and better peak shape was obtained in phosphate buffer solution. Therefore, phosphate buffer solution was adopted as supporting electrolyte in the following experiments.

Next, the voltammetric response of NHDC (3×10^{-6} mol L^{-1}) at the SWNTs/GCE with pH varying from 2.0 to 7.0 was investigated and every scan was performed for two cycles. Fig. 6A showed the half branch of the first cycle (getting P1 data) and Fig. 6B was the entire second cycle (getting P2 and P3 data). The voltammograms illustrated the highest response of current was obtained at pH 3.0, so the pH of 3.0 solution was selected for further experiments. As can be seen in Fig. 6C, the peak potentials shifted towards negatively with pH increasing for P1, P2 and P3, indicating the redox reactions of NHDC were accompanied by proton transfer. The peak potentials changed linearly with pH corresponding to equations of E_{p1} = -0.0384 pH + 0.7768 (R = 0.996), E_{p2} = -0.0577 pH + 0.6036 (R = 0.997) and E_{p3} = -0.0604 pH + 0.5667 (R = 0.998), respectively. The slope of 0.0384V/pH for P1 elucidated the process of P1 involved

protons and electrons in a ratio of 1:2. The slopes of0.0577V/pH for P2 and 0.0604V/pH for P3 were close to Nernstian slope of 0.059V/pH at 25℃, suggesting the same numbers of electrons and protons are involved in the redox reaction of P2 and P3.

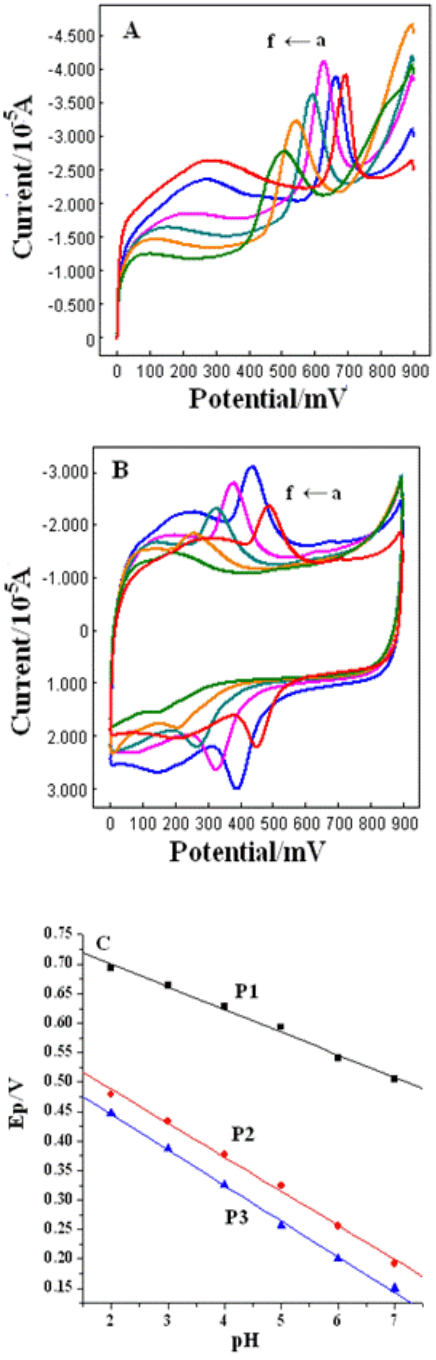

Fig 6. The effect of solution pH on the response of NHDC (3 ×10^{-6} mol L^{-1}) at SWNTs/GCE **(A)** The first half branch in the first cycle of voltammogram. **(B)** The entire second cycle of voltammogram.**(C)** pH-dependences of peak potential. pH of PBS: (from curve a to f): 2.0, 3.0, 4.0, 5.0, 6.0, 7.0. Other conditions were same as Fig. 4

Characteration of NHDC at different scan rates

To further elucidate the electrode reaction character, cyclic voltammetry with different scan rates was investigated in a 3×10^{-6} mol L^{-1} NHDC solution. Fig. 7A showed the superimposed voltammograms changing the scan rate from 0.02 V s^{-1} to 0.2 V s^{-1}. As it can be seen, the peak potentials of P1 and P3 shifted positively while P2 shifted negatively with scan rate increasing. For P1, there was a good linear relationship between log i_{p1} and log v corresponding to the following equation (shown in Fig. 7B): log i_{p1} (μA) = 0.830 log v (V/s) +2.361 (R=0.998). The slope value of 0.830 suggested that the anodic peak P1 was governed by both adsorption and diffusion. Meanwhile, a good linear relationship between the peak potential (E_{p1}) and ln v was also obtained with following regression equation: E_{p1} (V) = 0.0280 ln v (V s^{-1}) + 0.7505 (R=0.997). According to Laviron's theory [19] for an irreversible electrode process,, the relationship between E_p and scan rate could be expressed by the following equation:

$$E_p(\mathrm{V}) = E^{0'} - \frac{RT}{\alpha \mathrm{nF}} \ln v \frac{RTk_s}{\alpha nF} + \frac{RT}{\alpha nF} \ln v$$

Where α is transfer coefficient, k_s *i*s standard heterogeneous electron rate constant, n is electron transfer number involved in the rate determining step and $E^{0'}$ is formal potential; v, R, T and F have their usual significance. Thus, the value of n can be easily calculated to be 1.82 from the slope of E_{p1} vs ln$v$ by assuming α to be 0.5, which suggested that the two electrons were involved in P1 of NHDC. Based on the above mentioned equation, the charge transfer coefficient α and

heterogeneous electron rate constant k_s was calculated to be 0.46 and 1.07s^{-1}, respectively. Moreover, the formal potential $E^{0'}$(0.6527V) could be calculated through intercept of E_{p1} versus v plot on the ordinate by extrapolating the line to v = 0.

For P_2 and P_3, the peak currents grew with the increasing of scan rates and there were good linear relationships between i_p and v, corresponding to following equation: i_{p2} (μA)= 266.39 v (V s^{-1}) + 0.799 (R = 0.998) and i_{p3} (μA) = 239.11v (V s^{-1}) +1.403 (R = 0.998). This result demonstrated that the redox process of P2 and P3 was controlled by adsorption. With the scan rate increasing from 0.02 V s^{-1} to 0.20 V s^{-1}, the reduction peak potential (E_{p2}) was negatively shifted, and the oxidation peak potential (E_{p3}) was positively shifted with peak-to-peak separation (E_p) varying from 0.017 V s^{-1} to 0.109 V s^{-1}, indicating the increasing of redox irreversibility of P2 and P3. These data demonstrated that the redox of P2 and P3 was a quasi-reversible process driven by adsorption. The good linear relationships (Fig. 7C) were exhibited between peak potential and ln v and two liner regression equations were obtained as E_{p2} (V) = -0.0267 ln v(V s^{-1})+0.3156 (R = 0.98) and E_{p3} (V) = 0.0258 ln v (V s^{-1}) + 0.4974 (R = 0.98). According to above results, the electrontransfer kinetics of this reaction system can be obtained using the approach developed by Laviron' s equation [19],

$$E_{pc} = E^{0'} - \frac{RT}{\alpha nF}\ln v \qquad (1)$$

$$E_{pa} = E^{0'} - \frac{RT}{(1-\alpha)nF}\ln v \qquad (2)$$

$$\lg k_s = \alpha\lg(1-\alpha) + (1-\alpha)\lg\alpha - \lg\frac{RT}{nFv} - \alpha(1-\alpha)\frac{nF\Delta Ep}{2.3RT} \qquad (3)$$

where k_s, v, n, α, R, F, and T have their usual meaning. Then, a value of 2 could be achieved for n and α was 0.5 contained for P2 and P3 redox according to Eq. (1) and Eq. (2). Based on the Eq. (3), the value of heterogeneous electron rate constant ks was further calculated to be 0.81 s^{-1}.

Based on the experimental data and calculation results mentioned above, we can conclude that the redoxreaction of NHDC on SWNTs/GCE is a two-electron accompanying with one proton irreversible oxidation process first (P1) and following a two-electron and two-proton quasi-reversible redox process (P2 and P2). Thus, a reasonable electrochemical reaction mechanism was expressed as Scheme 1.

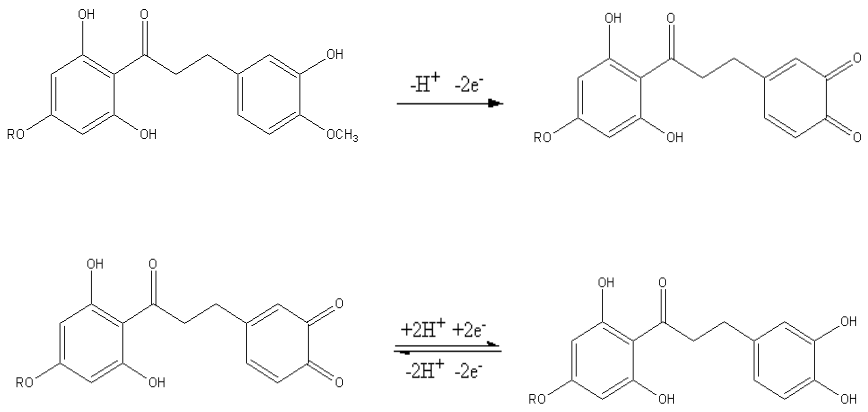

Scheme 1 Reaction mechanism of NHDC at SWNTs/GCE

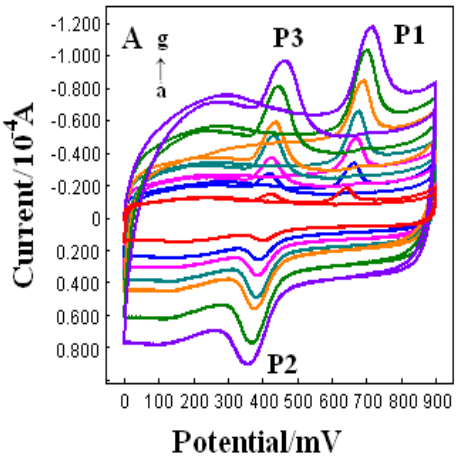

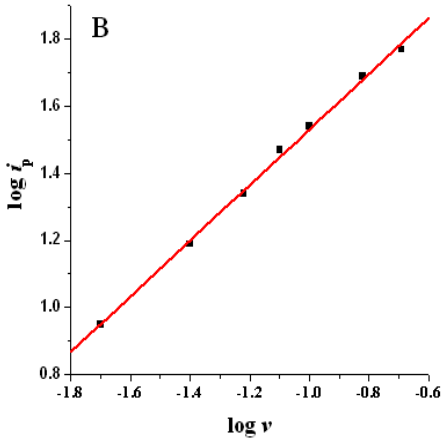

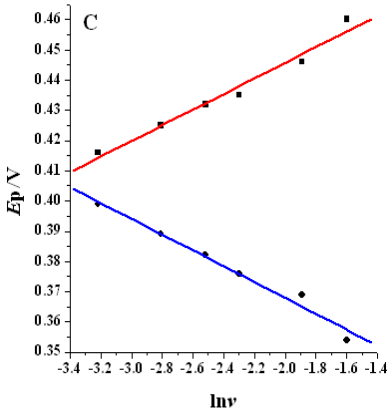

Fig. 7. Effect of scan rate on the response of NHDC (3×10^{-6} mol L^{-1}) at SWNTs/GCE **(A)** The superimposed voltammograms with different scan rate (from a to g): 0.02, 0.04,0.06, 0.08, 0.10, 0.15, 0.20 V s^{-1}. **(B)** The relationship of log i_{p1} against log v **(C)** The relationship between E_p and ln v, curve a for P2, curve b for P3. Other condition were same as Fig. 4

Chronocoulometry studies

For an mainly adsorption-controlled electrode process, it is necessary calculate the saturated absorption capacity (Γ_{max}) of a target compound on the electrode surface. For this system, multi-potential step chronocoulometry was employed for investigating the electrochemical processes. The SWNTs/GCE was immersed in a NHDC solutions

(3×10^{-6} mol L^{-1}) for 30min to achieve saturated absorption. And then, thrice step potentials from 0.50 to 0.90 V (first step), 0.90 to 0.0 V (second step) and 0.90 to 0.50 V (third step) were applied. The Q~t curve was recorded to calculate the saturated absorption capacity (Fig. 8A curve a1, a2, a3). For control, Q~t curve was recorded in blank PBS solution too (Fig. 8A curve a1', a2', a3'). The markers a1, a2 and a3 correspond with P1, P2 and P3 in Fig. 3 and the corresponding $Q\sim t^{1/2}$ plots were also performed and shown in Fig. 7B, C, D. At the first step, the corresponding $Q\sim t^{1/2}$ plots of b1, b1' were obtained with linear equations of Q (10^{-5} C) = 7.026 $t^{1/2}$ ($s^{1/2}$) +37.4934 and Q (10^{-5} C) = 2.519 $t^{1/2}$ ($s^{1/2}$) + 27.1749, respectively. Compared with b1', a bigger intercept and different slope were obtained from b, indicating that the oxidation of NHDC at P1 was mainly controlled by adsorption along with diffusion. According to the Anson equation given below [20], the value of Q_{ads} was calculated to be 1.032×10^{-4} C.

$$Q = \frac{2nFAC(Dt)^{1/2}}{\pi^{1/2}} + Q_{dl} + Q_{ads}$$

Here, Q_{dl} is double-layer charge, Q_{ads} is the Faradaic charge due to the oxidation of adsorbed NHDC. Using Laviron's theory of Q_{ads} = nFAΓ* and intercepts for curves b1 and b1', a Γ* value of 7.531×10^{-9} mol/cm^2 was obtained. Meanwhile, the diffusion coefficient (D) was calculated to be 2.2×10^{-6} cm^2/s from the slope of curve b1.

From the next two potential steps, the corresponding $Q\sim t^{1/2}$ were also performed and shown in Fig.7 C, D. As displayed, the control and NHDC plots have same slope values, which provided additional evidence of an adsorption-driven electrode process. Based on the equation mentioned above, the saturated absorption capacity for the oxidative and reductive of NHDC were calculated to be 1.51×10^{-8}mol/cm^2 and 8.88×10^{-9}mol/cm^2, respectively.

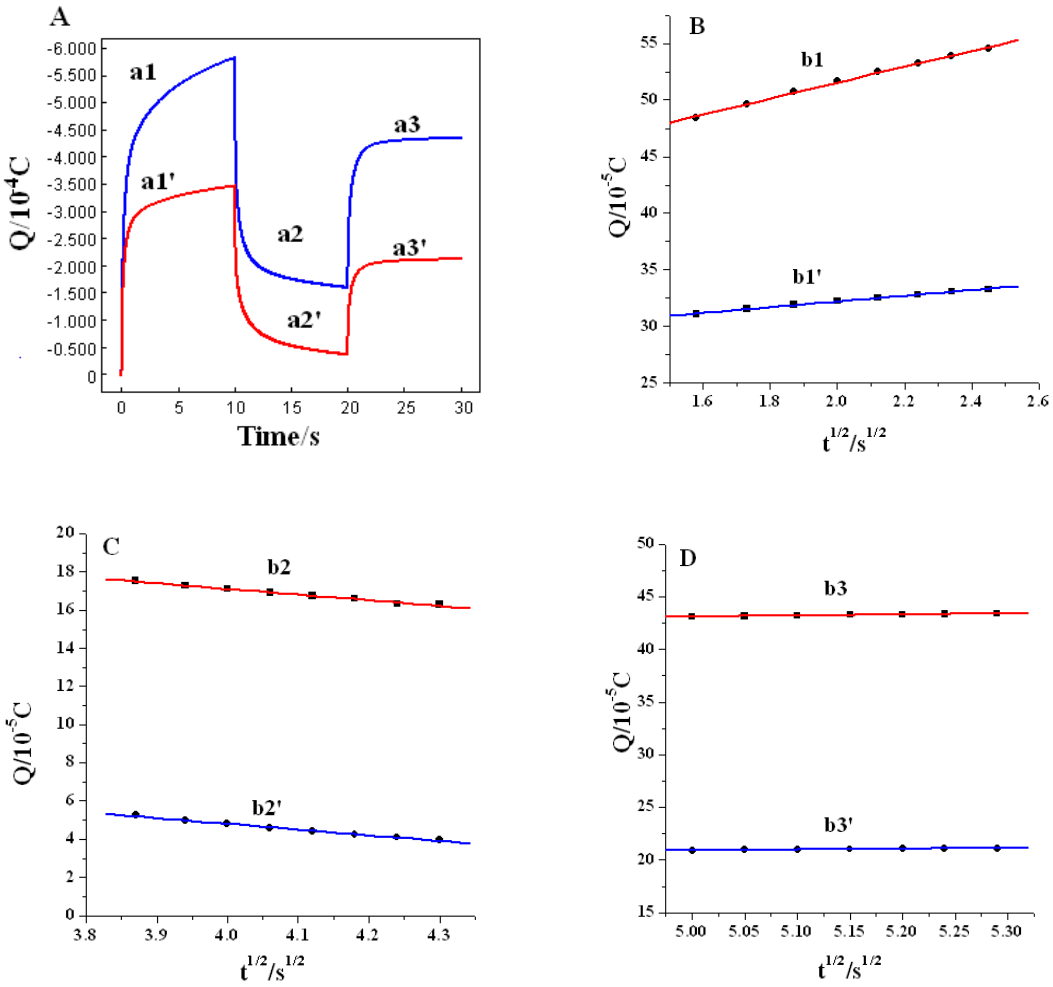

Fig. 8 (A) Chronocoulometric responses curves obtained in the absence (curve a1', a2', a3') and presence (curve a1, a2, a3) of 3×10^{-6} mol L^{-1} NHDC. **(B-D)** the relationship of charge Q vs. $t^{1/2}$, corresponding data were derived from (A)

Analytical applications and methods validation

Optimization of accumulation conditions

In consideration of the detection sensitivity and adsorption of NHDC on the SWNTs/GCE surface, effects of accumulation time and potential on the peak current were studied. For a NHDC solution (5×10^{-7} mol L^{-1}), the anodic current of P1 increased with the increasing of accumulation time t_{acc} and then reached a maximum value when t_{acc} was above 180s. So the t_{acc} of 180 s was used for further studies. After investigation, the accumulation potential had little effect on the anodic current in the range of -0.1-0.6V and open circuit. Thus, accumulation of NHDC was carried out under open circuit in the following experiments.

Calibration curve, stability and reproducibility

In this study, the current response of P1 was selected to establish calibration curve due to better sensitiveness. Fig. 9A displayed the responses of NHDC with different concentration under optimized working conditions by LSV using SWNTs/GCE. A good relationship could be obtained between peak current (i_p) and NHDC concentrations in the range of 5×10^{-8} mol/L-8×10^{-6} mol/L (shown in Fig. 9B). The linear regression equation was i_p (10^{-6}A) = 5.0947C

(μmol L^{-1}) +3.8403 (R= 0.996) with a detection limit of 2× 10^{-8} mol/L. Here, the detection limit was the concentration being able to give the measurable signal that can be observed by naked eye.

To estimate the reproducibility of the proposed sensor, five successive CV in 3×10^{-6} mol L^{-1} NHDC solution were recorded and the obtained relative standard deviation (RSD) was 4.98%, At the same time, the fabrication reproducibility was also studied by constructing five modified electrodes in parallel under the same condition and the measured RSD was 3.16%. When stored in 4 □ in a refrigerator, the modified electrode retained 96.2% of the initial response after two weeks. These experiments indicated that the proposed electrode had good stability and repeatability for the determination of NHDC.

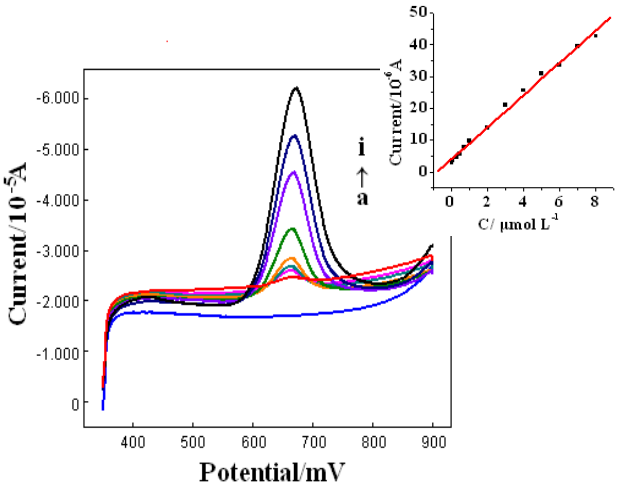

Fig. 9 LCV curves of NHDC with different concentrations NHDC concentrations (from curve a to i): 0, 5×10^{-8}, 3×10^{-7}, 5×10^{-7}, 7×10^{-7}, 2×10^{-6}, 4×10^{-6}, 6×10^{-6}, 8×10^{-6}mol/L. Supporting electrolyte: 0.1mol L^{-1} PBS (pH=3.0), Scan rate: 50 mV s^{-1}, Open-circuit accumulation time: 180 s. The insert was the i_p vs C_{NHDC} plot

Interference studies

In consideration of the possible analytical application for proposed method, the interferential experiments were evaluated primarily aiming at some food and beverage samples. Experiments were performed in a NHDC (1×10^{-6}mol L^{-1}) solution spiked with various excess amounts of these species under the same experimental conditions. The tolerance limit for foreign species was taken as the largest amount yielding a relative error ≤ 5% for the determination of NHDC. The results indicated that 200-fold Ca^{2+}, Cu^{2+}, Mg^{2+}, Mn^{2+}, Fe^{2+}, 50-fold glucose, sucrose, amylum, citrate acid, sodium citrate, oxalic acid, vitamin E, vitamin C, vitamin B_2 and edetate disodium caused negligible interference in the quantitative analysis of NHDC, which clearly proved the reasonable selectivity for the proposed method.

Analysis of samples

To evaluate the practical applicability of the proposed method, one commercially available beverage was employed to determine the NHDC content. Firstly, the beverage was under sounding for several minutes to remove carbon dioxide, and then appropriate amount of beverage (1.2247g) was added in the supporting electrolyte for determination. The recovery was calculated afterwards by adding some standard NHDC solutions into the sample. The results, listed in Table 1, showed that the content of NHDC in detected commercially beverage was 0.320mg/kg, and the recovery evaluated was between 93.15% and 109.23%. which demonstrated the method's efficiency and applicability

Table 1 Determination of NHDC in commercially available beverage

Original found [a] (μmol L^{-1})	Standard added (μmol L^{-1})	Total found [a] (μmol L^{-1})	RSD (%)	Recovery (%)	Content of NHDC in beverage (mg/kg)
0.064	1.5	1.574	2.6	100.63	0.320
	2.0	3.893	3.8	109.23	
	2.0	5.183	1.7	93.15	

[a] **average value of three replicate measurements.**

Conclusion

In conclusion, an electrochemical sensor based on SWNTs modified electrode was fabricated for the detection of trace amounts of NHDC. Using this sensor, the electrochemical properties of NHDC were investigated in detail for the first time and dynamic parameters of electrode process were also calculated. The modified electrode improved the electrochemical response of NHDC and exhibited good sensitivity with the detection limit of 2×10^{-8} mol L^{-1} by LSV under accumulation time of 180s. Furthermore, the proposed method provided convenient application for determination of NHDC and could be applied for the detection in commercially available beverage with satisfactory results.

Acknowledges

The authors really appreciate for the financial support from the National Natural Science Foundation of China (Grant Nos. 21275132 & 20775073).

Notes and references

College of Chemistry and Molecular Engineering, Zhengzhou University, Zhengzhou 450001, PR China. Corresponding author. Tel.: +86 0371 67781757; fax: +86 0371 67763654; E-mail address: yebx@zzu.edu.cn

1 R. H. Horowitz, B. Gentili, *Tetrahedron,* 1963, **19**, 773.

2 R. M. Horowitz, B. Gentili, Dihydrochalcone sweeteners from citrus flavanones, ed. R. C. Gelardi, Marcel Dekker, New York, 2nd edn., 1991, pp. 97–115.

3 D. H. Choi, N.A. Kim, T. S. Nam, et al., *Drug Dev Ind Pharm,*2004, **40**, 308.

4 H. Hellal, *Feed International,* 2004, **24**, 16.

5 D. H. Waalkens-Berendsen, M. E. Kuilman-Wahls, A. Bar, *Regulatory Toxicology and Pharmacology*, 2004, **40**, 74.

6 Y. Li, J. Liu, R. Cao, et al., *J. Chem. Eng. Data,* 2013, **58**, 2527.

7 X. Li, H. Xiao, X. Liang, D. Shi, J. Liu, *J. Pharm. Biomed. Anal,* 2004, **34**, 159.

8 D. Y. Zhou, Q. Xu, X. Y. Xue, F. F. Zhang, X. M. Liang, *J. Pharm. Biomed. Anal,* 2006, **42,** 441.

9 F. A. Tomas-Barberan, F. Borrego, F. Ferreres, M. G. Lindley, *Food Chemistry,* 1995, **52**, 263.

10 A. Wasik, J. McCourt, M. Buchgraber, *Journal of Chromatography A,* 2007, **1157**, 187.

11 A. Zygler, A. Wasik, A. Kot-Wasik, et al., *Anal Bioanal Chem,* 2011, **400**, 2159.

12 M. G. Kokotou, N. S. Thomaidis, *Analytical Methods,* 2013, **5**, 3825.

13 T. Perea-Ruiz, C. Martinez-Lozano, V. Tomfis, et al., *Chromatographia,* 2000, **51**, 385.

14 S. Iijima, *Nature,* 1991, **354**, 56.

15 S. Iijima, T. Ichihashi, *Nature,* 1993, **363**, 603.

16 J. Zhang, X. Tan, D. Zhao, et al., *Electrochimica Acta,* 2010, **55**, 2522.

17 A. Gholizadeh, S. Shahrokhian, S. Mohajerzadeh, *Anal.Chem,* 2012, **84**, 5932.

18 N. S. Lawrence, R. P. Deo, J. Wang, *Anal Chim Acta,* 2004, **517,**131.

19 E. Laviron, *J. Electroanal. Chem,* 1979, **101**, 19.

20 F. C. Anson, *Anal. Chem,* 1964, **36**, 932.